PAPER

The optical Tamm states at the interface between a photonic crystal and nanoporous silver

IOP Publishing Journal of Optics
J. Opt. 19 (2017) 015104 (6pp) doi:10.1088/2040-8986/19/1/015104

The optical Tamm states at the interface between a photonic crystal and nanoporous silver

R G Bikbaev[1], S Ya Vetrov[1,2] and I V Timofeev[1,2]

[1] Siberian Federal University, Krasnoyarsk, 660041 Russia
[2] Kirensky Institute of Physics, Federal Research Center KSC SB RAS, 660036 Russia

E-mail: rashid-bikbaev@mail.ru

Received 6 October 2016, revised 14 November 2016
Accepted for publication 24 November 2016
Published 13 December 2016

Abstract

The optical Tamm states (OTSs) localized at the edges of a photonic crystal bounded by a nanoporous silver (NPS) film are investigated. NPS involves spherical vacuum nanopores dispersed in the metal matrix and is characterized by the effective resonance permittivity. The transmission, reflection, and absorption spectra of the structures under study at the normal incidence of light are calculated. It is shown that each Tamm state has its own frequency range where the real part of effective permittivity is negative. The light field localization at the high- and low-frequency OTSs is investigated. The specific features of spectral manifestation of the OTSs are studied in dependence on the nanopore concentration in the metal matrix and on the NPS film thickness.

Keywords: photonic crystal, nanoporous silver, optical Tamm state, effective permittivity

(Some figures may appear in colour only in the online journal)

Introduction

In recent years, there has been an increased interest in a special type of surface electromagnetic state excited at the normal incidence of light that are called the optical Tamm states (OTSs) [1, 2]. Such states are analogous to the Tamm surface states in physics of condensed matter. They can be excited between two photonic crystals with overlapping band gaps [3] or between a photonic crystal (PC) and a medium with negative permittivity ε [4]. The surface electromagnetic wave at the interface between the PC and the medium with $\varepsilon < 0$ is a single unit with the surface plasmon, i.e., oscillations of free electrons near the conductor surface. In experiments, the OTS manifests itself as a narrow peak in the transmission spectrum of a sample [5, 6].

The OTSs can be used in sensors and optical switches [7], Faraday- and Kerr-effect amplifiers [6, 8], organic solar cells [9], and absorbers [10]. Symonds *et al* [11] experimentally showed a laser based on the Tamm structure consisting of quantum wells embedded in a Bragg reflector with the silver-coated surface. Gazzano *et al* demonstrated the possibility of implementation of a single-photon source on the basis of confined Tamm plasmon modes [12]. The OTSs in magnetophotonic crystals were investigated in [6, 13−15]. Gessler *et al* [16] investigated the electro-optically tunable Tamm plasmon exciton polaritons. Savelev *et al* [17] predicted that the edges of a finite one-dimensional array of dielectric nanoparticles with the high refractive index can sustain the damped OTSs. Treshin *et al* [18] proposed and implemented the extremely high-efficiency transmission of light through a nanohole in a gold film, which was placed in the light field localized at the interface between the film and a one-dimensional PC. This effect is related to the field amplification at the interface between the superlattice and metal film due to the occurrence of the OTS. The hybrid states were studied in [19, 20]. In [21], the analog of the surface state in a structure containing a cholesteric liquid crystal was found. It was shown that the condition for the existence of this state is the presence of a quarter-wavelength layer between the crystal and metal, which is explained by the polarization properties of cholesterics different from the properties of scalar structures. Later on, the chiral OTS was found in a cholesteric liquid crystal [22]. As a metal layer, the authors used a mirror made of an anisotropic metal-dielectric

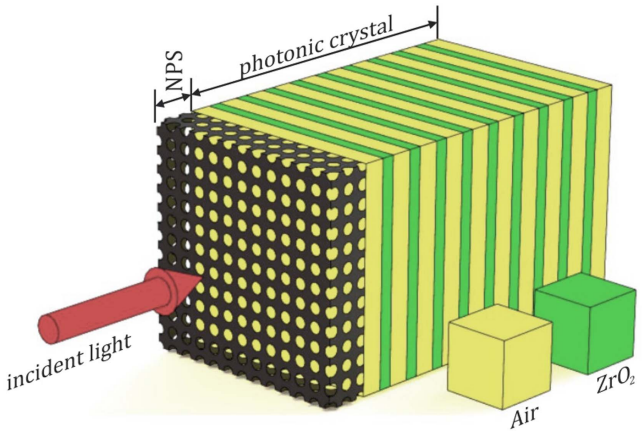

Figure 1. Schematic of a 1D PC conjugated with the nanoporous silver layer.

nanocomposite, which preserves polarization at reflection [23]. Such a nanocomposite contains metallic particles of spheroidal shape dispersed inside a transparent matrix. Its characteristic feature is the resonance in the frequency dependence of the effective dielectric constant due to the surface plasmon resonance in metal nanoparticles. Propagation of surface waves of plasmon polariton type at the boundary of dielectric medium and nanocomposite with silver inclusions of spherical shape are studied in [24]. OTS at the edges of the PC bounded by a nanocomposite with silver nanoparticles characterized by the resonant effective dielectric constant is explored in [25].

In addition, of great interest are the silicon-based porous structures [26] and plasmon materials, including silver and gold. These structures are fabricated using the chemical technique [27], electrochemical technique [28], and pulsed laser deposition in vacuum [29]. It should be noted that the pulsed laser deposition yields films with a thickness of up to 100 nm with spherical pores randomly dispersed in a matrix. Kaganovich *et al* [30] studied the polarization properties of such structures. In [29, 31] these films are shown to have the properties of both planar metal film and nanoparticles, respectively, demonstrating the excitation of surface plasmon-polariton resonance and surface resonance due to local plasmon resonances.

The aim of this study was to investigate the properties of the OTSs localized at the edges of a PC bounded by a nanoporous silver (NPS) film characterized by the effective resonance permittivity. NPS has two frequency ranges where the real part of its effective permittivity is negative. We demonstrate that the use of such a material makes it possible to obtain two OTSs inside one band gap. The spectral features of the observed OTSs are investigated in dependence on the structure parameters.

Description of the model and determination of transmission

The PC structure under study is a layered medium bounded by an NPS film on its one end (figure 1). A unit cell of the PC is formed from materials a and b with respective layers thicknesses d_a and d_b and permittivities ε_a and ε_b. The porous silver layer with thickness d_{NPS} contains spherical nanopores randomly distributed in the metal matrix.

Hereinafter, we assume the PC structure to be placed in vacuum. In accordance with the Maxwell−Garnett model, the effective permittivity is expressed as [32]

$$\varepsilon_{\mathrm{NPS}} = \varepsilon_M\left[1 + \frac{f(\varepsilon_d - \varepsilon_M)}{\varepsilon_M + (1-f)(\varepsilon_d - \varepsilon_M)1/3}\right], \quad (1)$$

where f is the filling factor, i.e., the fraction of nanopores in the matrix; ε_d and $\varepsilon_M(\omega)$ are the permittivities of the pores and metal matrix, respectively; and ω is the radiation frequency.

The permittivity of silver is determined using the Drude approximation

$$\varepsilon_M(\omega) = \varepsilon_0 - \frac{\omega_p^2}{\omega(\omega + \mathrm{i}\gamma)}, \quad (2)$$

where ε_0 is the constant that takes into account the contributions of interband transitions of bound electrons, ω_p is the plasma frequency, and γ is the reciprocal electron relaxation time.

Transmission of a planar light wave polarized along the x axis and propagating along the z direction was calculated using the transfer matrix technique [33]. The light field variation upon transmission through each layer of the structure is determined by the second-order transfer matrix. The transfer matrix of the entire structure, which relates amplitudes of the incident and transmitted waves, is a product of 2×2 matrices

$$M = T_{01}T_{12}...T_{N-1,N}T_{N,S}, \quad (3)$$

where the transfer matrix is

$$T_{n-1,n} = \frac{1}{2}\begin{pmatrix}(1+h)\mathrm{e}^{-\mathrm{i}\alpha_n\gamma_n} & (1-h)\mathrm{e}^{\mathrm{i}\alpha_n\gamma_n}\\ (1-h)\mathrm{e}^{-\mathrm{i}\alpha_n\gamma_n} & (1+h)\mathrm{e}^{\mathrm{i}\alpha_n\gamma_n}\end{pmatrix}, \quad (4)$$

here, $h = (\varepsilon_n/\varepsilon_{n-1})^{1/2}$, $\varepsilon(n)$ is the permittivity of the n layer, $\alpha_n = (\omega/c)\varepsilon(n)^{1/2}$, c—is the speed of light, and $\gamma_n = z_n - z_{n-1}$ is the layer thicknesses, where $n = 1, 2, \ldots, N$, z_n is the coordinate of the interface between the n layer and the $(n+1)$ layer adjacent from the right ($\gamma_{N+1} = 0$). The transfer matrix for the orthogonally polarized wave is obtained from equation (6) by substituting $(\varepsilon_{n-1}/\varepsilon_n)^{1/2}$ for h. The energy coefficients of transmittance, reflectance, and absorbance are determined using the respective formulas

$$T(\omega) = \frac{1}{|\hat{M}_{11}|^2},\ R(\omega) = \frac{|\hat{M}_{11}|^2}{|\hat{M}_{21}|^2},\qquad A(\omega) = 1 - T(\omega) - R(\omega). \quad (5)$$

Here, $\hat{M}_{11}$ and $\hat{M}_{21}$ are the elements of matrix $\hat{M}$.

Results and discussion

Let us consider the OTSs implemented in the form of standing surface waves localized at the interface between the PC and isotropic NPS layer. NPS is characterized by the

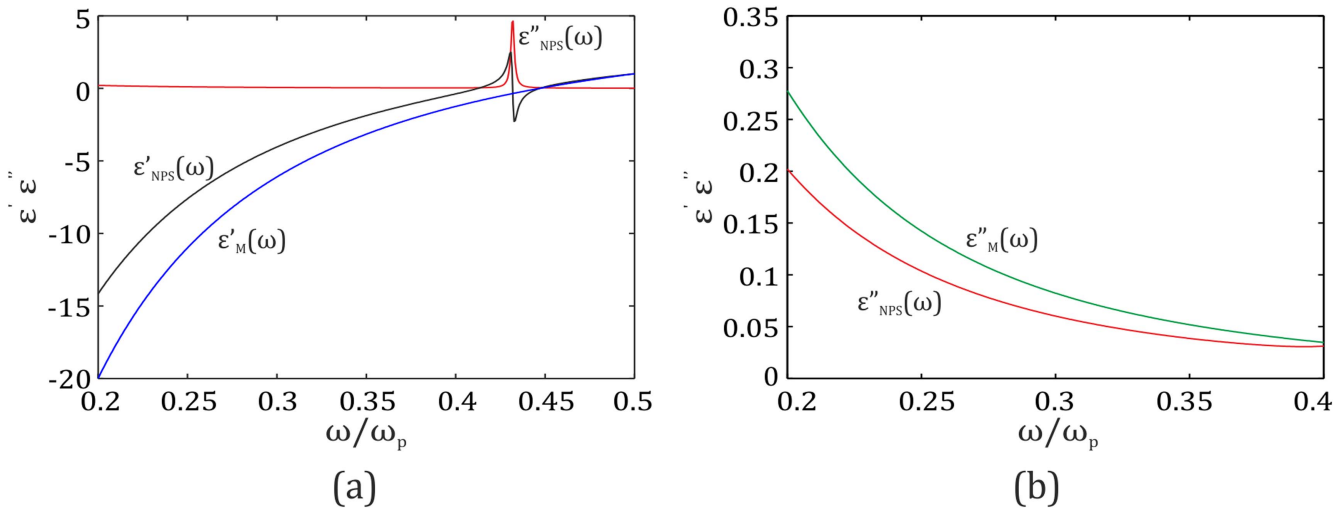

Figure 2. (a) Dependences of the imaginary ($\varepsilon''(\omega)$) and real ($\varepsilon'(\omega)$) parts of effective permittivity on normalized frequency ω/ω_p for silver ($\varepsilon_M(\omega)$) and nanoporous silver ($\varepsilon_{\mathrm{NPS}}(\omega)$) with a filling factor of $f = 0.2$. (b) The $\varepsilon''_{\mathrm{NPS}}(\omega)$ and $\varepsilon''_M(\omega)$ values in the vicinity of the first band gap of the initial photonic crystal (see figure 3(a)).

effective complex permittivity $\varepsilon_{\mathrm{NPS}}(\omega)$

$$\varepsilon_{\mathrm{NPS}}(\omega) = \varepsilon'_{\mathrm{NPS}}(\omega) + \mathrm{i}\varepsilon''_{\mathrm{NPS}}(\omega). \tag{6}$$

For certainty, we will investigate zirconium dioxide ZrO_2 with the permittivity $\varepsilon_b = 4.16$ and vacuum with the permittivity $\varepsilon_a = 1$ as materials of alternating layers. The layer thicknesses are $d_a = 100$ nm and $d_b = 40$ nm and the number of layers is $N = 11$.

The NPS layer with a thickness of $d_{\mathrm{NPS}} = 100$ nm is a metal matrix with uniformly distributed vacuum pores with $\varepsilon_d = 1$. The parameters of silver are $\varepsilon_0 = 5$, $\omega_p = 9$ eV, and $\gamma = 0.02$ eV. The frequency dependences of the real and imaginary parts of permittivity calculated using formula (1) show that the frequency ω corresponding to the resonance in the defect layer shifts toward higher frequencies with an increase in the volume concentration of nanopores. In this case, the half-width of the resonance curve $\varepsilon''_{\mathrm{NPS}}(\omega)$ changes insignificantly, the curve $\varepsilon'_{\mathrm{NPS}}(\omega)$ is noticeably modified, and the frequency range at which $\varepsilon'_{\mathrm{NPS}}(\omega) < 0$ narrows. As an example, figure 2(a) shows the dependences $\varepsilon'(\omega)$ and $\varepsilon''(\omega)$ for silver and porous silver with a filling factor of $f = 0.2$. The resonance observed at a frequency of $\omega = 0.4321\omega_p$ with a corresponding wavelength of $\lambda = 317.7$ nm is caused by the plasmon resonance on the surface of individual nanopores [34].

Descending the real part of the complex permittivity of the NPS, at frequencies below $\omega = 0{,}4321\omega_p$, is a consequence of growth in the contribution of the second term in (2) in the dielectric constant of silver.

It should be noted also that the imaginary part of complex permittivity in the frequency range from $0.2\omega/\omega_p$ to $0.4\omega/\omega_p$ for NPS acquires the values smaller than the imaginary part of permittivity of ordinary silver and, as a consequence, weakens dissipations in the system (figure 2(b)).

The transmission spectrum for the structure with an NPS layer thickness of $d_{\mathrm{NPS}} = 100$ nm and a filling factor of $f = 0.1$ is presented in figure 3(a).

It can be seen that two transmission peaks are formed inside the band gap at frequencies of $\omega_1 = 0.4177\omega_p$ and $\omega_2 = 0.437\omega_p$. At the wavelength of the transmission peak the light field is localized at the boundary between the PC and NPS layer and exponentially decreases in either direction. In fact, the light keeps locked between two mirrors—Bragg and metal, since the OTS wavelength falls into the bang gap of the PC and in the region of negative values of the real part of the NPS effective permittivity. Each Tamm state corresponds to a frequency range with a negative real part of the complex dielectric constant (figure 2(a)). High-frequency peak is caused by localized plasmons near the nanopore, the low-frequency peak corresponds to the excitation of OTS on the border of the metal layer and the PC.

The permittivities of porous silver at these frequencies are $\varepsilon_{\mathrm{NPS}}(\omega_1) = -0.1369 + 0.0549\mathrm{i}$ and $\varepsilon_{\mathrm{NPS}}(\omega_2) = -0.4448 + 0.0846\mathrm{i}$, respectively. The established OTSs exist only in very narrow frequency ranges, where the real part of effective permittivity of NPS acquires negative values.

The low transmittance at the OTS frequencies is explained by the fairly strong absorption of the NPS layer and, consequently, low reflectance at the corresponding frequencies.

At the frequency ω_1 absorptance and reflectance of incident radiation are 62.7% and 34.5%. For frequency ω_2 these values are 92.5% and 0.85% respectively. Such a strong absorption in a narrow frequency range is due to plasmon resonance on the surface of the nanopore. Additional central peak at the frequency $\omega = 0.4282\omega_p$ in the absorption spectrum of the NPS-PC structure corresponds to the resonant frequency of effective dielectric permittivities (figure 2(a)).

The local intensity distribution for the modes with the frequencies corresponding to the Tamm states is illustrated in figure 4.

It can be seen that the light field localization at the high-frequency OTS exceeds the localization at the low-frequency OTS by 40%. Note also that the light field in the OTS is

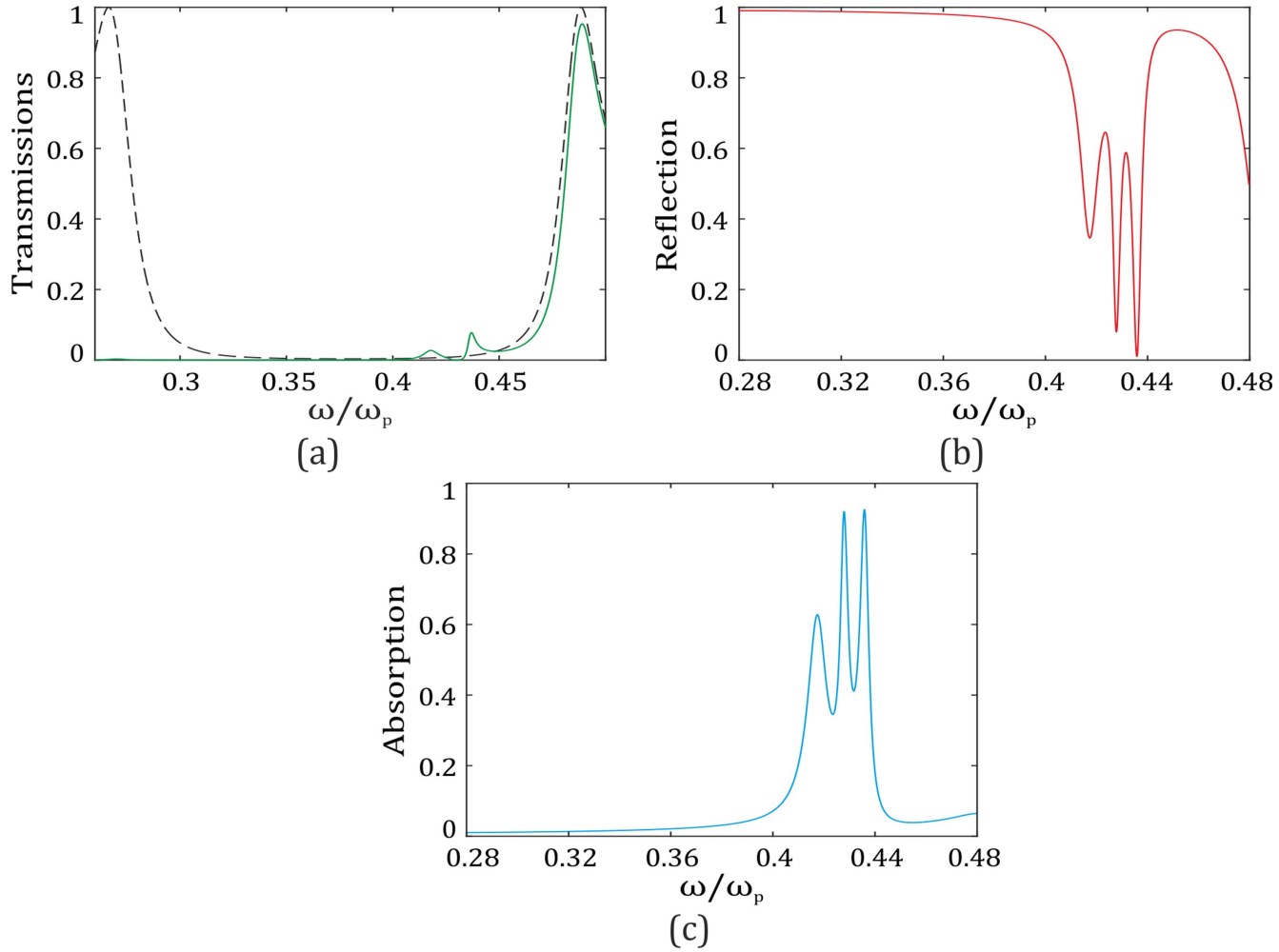

Figure 3. Transmission spectra of (a) the initial PC (long-dash line) and PC conjugated with the porous silver layer (solid line), (b) reflection spectra, and (c) absorption spectra of the NPS-PC system at $\varepsilon_b = 4.16$ and $\varepsilon_a = 1$. The respective layer thicknesses are $d_a = 100$ nm and $d_b = 40$ nm. The NPS layer thickness is $d_{\mathrm{NPS}} = 100$ nm and the filling factor is $f = 0.1$.

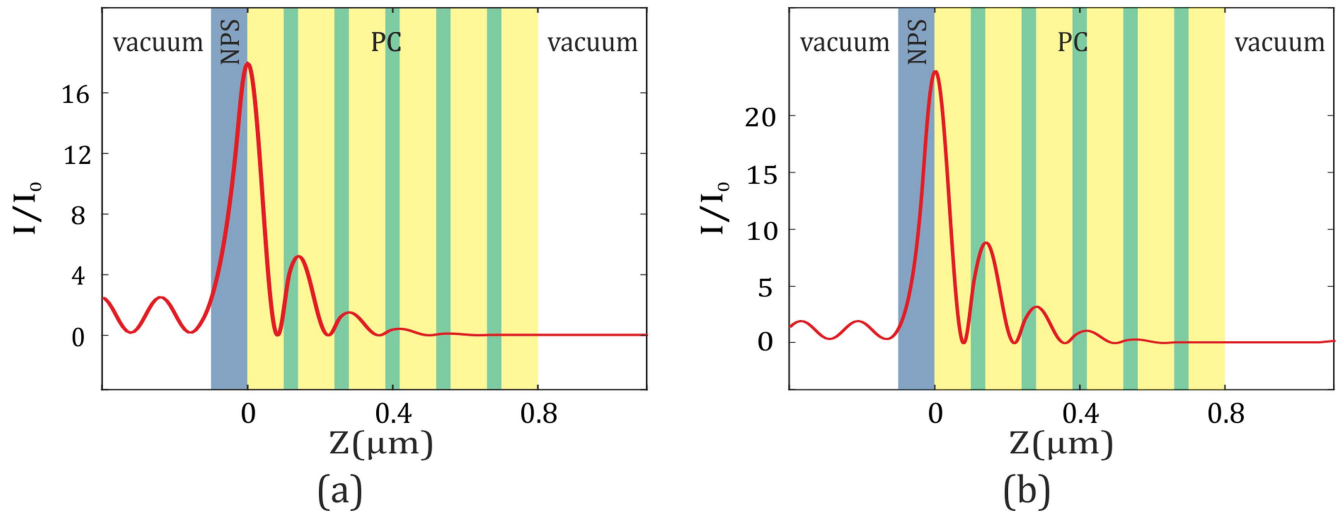

Figure 4. Field intensity distribution for (a) the low- and (b) high-frequency OTSs. Color vertical bands show the positions of layers of the 1D PC and conjugated nanoporous silver layer.

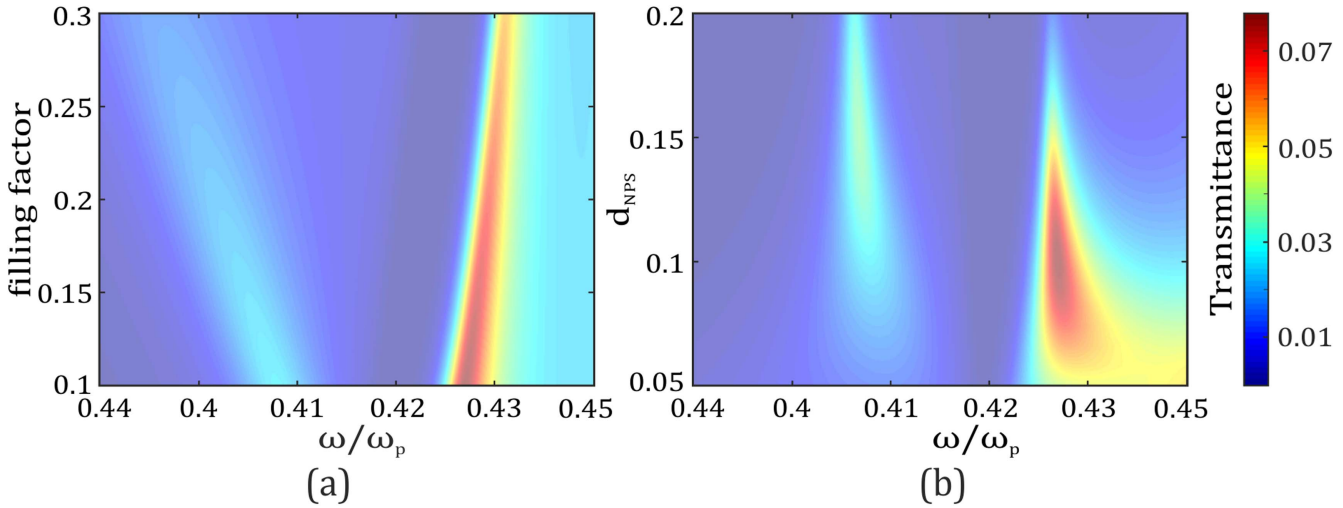

Figure 5. Transmission spectra of the NPS-PC structure (a) at different filling factors and fixed thickness $d_{NPS} = 100$ nm and (b) at different NPS layer thicknesses and fixed filling factor $f = 0.1$. The color bar corresponds to both figures.

localized in the region comparable with the wavelength. Such a model with two highly localized states with close frequencies can be used to design a laser based on the OTSs [35, 36]. In recent years, two- [37] and three-mode lasers [38] attract much attention. In the model proposed by us, in contrast to the model described in [37], modes are insensitive to the polarization of incident light, so they can be observed simultaneously.

The observed OTSs are extremely sensitive to the filling factor and NPS layer thickness, since the transmission peaks are very close to the plasmon resonance on the pore surface and, consequently, to the absorption band of porous silver.

The transmission spectra of the structure under study at different filling factors and NPS layer thicknesses are shown in figure 5.

Note that the growth of the filling factor leads to repulsion of the OTS frequencies (figure 5(a)). The calculations show that such a behavior of the OTS frequencies is caused by an increase in the degree of overlap of the localized mode fields.

In this case, the transmission at the OTS frequencies drops due to an increase in the absorption by NPS. Therefore, to obtain two Tamm states, it is favorable to use weakly porous silver structures with a filling factor of $f \approx 0.1$.

Variation in the NPS film thickness does not lead to the frequency shift of the Tamm states and affects only the transmission at their frequencies. In this case, the maximum transmission at the OTS frequency for the low-frequency peak is attained at a film thickness of $d_{NPS} = 152$ nm and for the high-frequency peak, at $d_{NPS} = 97$ nm (figure 5(b)).

Conclusions

We investigated the spectral properties of a 1D PC bounded by a resonantly absorbing NPS layer thickness consisting of a silver matrix with spherical nanopores. The results were obtained using the transfer matrix technique. The spectral manifestation of the OTS is caused by the negative effective resonance permittivity of the NPS layer in the visible spectral range.

For the first time, two Tamm states were obtained inside the initial photonic crystal with the use of the NPS film. It was demonstrated that each Tamm state has its own frequency range with the negative real part of effective permittivity. The light field localization at the OTS frequencies was studied.

In the case of a planar metal film (filling factor $f = 0$) in the transmission spectrum of the structure, as expected, there is a single peak corresponding to the excitation of OTS.

The spectral dependence of the Tamm states on the filing factor of the NPS film was obtained. It was established that an increase in the filing factor leads to an increase in the frequency distance between the transmission peaks corresponding to the OTSs. The dependence of the transmission spectrum of the photonic-crystal structure in the NPS film thickness was studied. It was demonstrated that the growth of the filling factor leads to repulsion of the OTS frequencies and that such a behavior of the OTS frequencies is caused by an increase in the degree of overlap of the localized mode fields. The results can be used for two-mode lasing through OTS.

Acknowledgments

The reported study was funded by Russian Foundation for Basic Research, Government of Krasnoyarsk Territory, Krasnoyarsk Region Science and Technology Support Fund to the research project № 16-42-243065, SB RAS No. II.2P (0358-2015-0010), the Ministry of Education and Science of the Russian Federation, projects no. 3.1276.2014/K and no. 3.1211.2017/PCH. I.V.T. acknowledges financial support from RFBR research project № 15-02-03838.

References

[1] Vinogradov P, Dorofeenko A V, Merzlikin A M and Lisyansky A A 2010 *Phys. Usp.* **53** 243–56

[2] Kavokin V, Shelykh I and Malpuech G 2005 *Appl. Phys. Lett.* **87** 261105
[3] Kavokin V, Shelykh I and Malpuech G 2005 *Phys. Rev.* B **72** 233102
[4] Kaliteevski M, Iorsh I, Brand S, Abram R A, Chamberlain J M, Kavokin A V and Shelykh I A 2007 *Phys. Rev.* B **76** 165415
[5] Sasin M E, Seisyan R P, Kalitteevski M A, Brand S, Abram R A, Chamberlain J M, Egorov A Y, Vasil'ev A P, Mikhrin V S and Kavokin A V 2008 *Appl. Phys. Lett.* **92** 251112
[6] Goto T, Dorofeenko A V, Merzlikin A M, Baryshev A V, Vinogradov A P, Inoue M, Lisyansky A A and Granovsky A B 2008 *Phys. Rev. Lett.* **101** 113902
[7] Zhang W L and Yu S F 2010 *Opt. Commun.* **283** 2622–6
[8] Vinogradov P, Dorofeenko A V, Erokhin S G, Inoue M, Lisyansky A A, Merzlikin A M and Granovsky A B 2006 *Phys. Rev.* B **74** 045128
[9] Zhang X-L, Song J-F, Li X-B, Feng J and Sun H-B 2012 *Appl. Phys. Lett.* **101** 243901
[10] Gong Y, Liu X, Lu H, Wang L and Wang G 2011 *Opt. Express* **19** 18393
[11] Symonds C, Lheureux G, Hugonin J P, Greffet J J, Laverdant J, Brucoli G, Lemaitre A, Senellart P and Bellessa J 2013 *Nano Lett.* **13** 3179
[12] Gazzano O, Michaelis de Vasconcellos S, Gauthron K, Symonds C, Voisin P, Bellessa J, Lemaître A and Senellart P 2012 *Appl. Phys. Lett.* **100** 232111
[13] Dong H Y, Wang J and Cui T J 2013 *Phys. Rev.* B **87** 045406
[14] Da H, Bao Q, Sanaei R, Teng J, Loh K P, Garcia-Vidal F J and Qiu W 2013 *Phys. Rev.* B **88** 205405
[15] Khokhlov N E *et al* 2015 *J. Phys. D: Appl. Phys.* **48** 095001
[16] Gessler J, Baumann V, Emmerling M, Amthor M, Winkler K, Höfling S, Schneider C and Kamp M 2014 *Appl. Phys. Lett.* **105** 181107
[17] Savelev R S, Miroshnichenko A E, Sukhorukov A A and Kivshar Y S 2014 *JETP Lett.* **100** 430
[18] Treshin V and Klimov V V 2013 *Phys. Rev.* A **88** 023832
[19] Afinogenov B I, Bessonov V O, Nikulin A A and Fedyanin A A 2013 *Appl. Phys. Lett.* **103** 061112
[20] Fang Y-T *et al* 2014 *Opt. Commun.* **320** 99–104
[21] Vetrov S Y, Pyatnov M V and Timofeev I V 2014 *Opt. Lett.* **39** 2743
[22] Timofeev I V and Vetrov S Y 2016 *JETP Lett.* **104** 380–3
[23] Rudakova N V, Timofeev I V and Vetrov S Y 2017 *Bull. Russ. Acad. Sci.: Phys.* **81** 10–4
[24] Filatov L D, Sannikov D G, Semencov D I and Evseev D A 2014 *Phys. Solid State* **56** 1424–30
[25] Vetrov S Y, Bikbaev R G and Timofeev I V 2013 *J. Exp. Theor. Phys.* **117** 988–98
[26] Golovan L A, Timoshenko V Y and Kashkarov P K 2007 *Phys. Usp.* **6** 619–38
[27] Kim B, Hong S C, Jung S, Nam J, Bang J and Kim S 2013 *Chem. Phys. Chem.* **14** 2663–6
[28] Yeh F, Tai C, Huang J and Sun I 2006 *J. Phys. Chem.* B **110** 5212–22
[29] Kaganovich E *et al* 2012 *Nanosyst. Nanomater, Nanotechnol.* **10** 859–67
[30] Kaganovich E, Kravchenko S, Maksimenko L, Manoilov E, Matyash I, Mishchuk O, Rudenko S and Serdega B 2011 *Opt. Spectrosc.* **110** 513–21
[31] Rudenko S, Stetsenko O, Krischenko I, Maksimenko L, Kaganovich E and Serdega B 2016 *Opt. Spectrosc.* **120** 540–5
[32] Maxwell Garnett J C 1904 *Phil. Trans. R. Soc.* **203** 385–420
[33] Yeh P 1979 *J. Opt. Soc. Am.* **69** 742
[34] Sihvola 2008 *Electromagnetic Mixing Formulas and Applications* (London: Institution of Engineering and Technology) p 284 http://amazon.com/o/ASIN/0852967721
[35] Zhang Z, Li Y, Liu W, Sun Y, Jiang H and Chen H 2016 *J. Opt.* **18** 025103
[36] Symonds C, Lheureux G, Hugonin J P, Greffet J J, Laverdant J, Brucoli G, Lemaitre A, Senellart P and Bellessa J 2013 *Nano Lett.* **13** 3179–84
[37] Lheureux G, Azzini S, Symonds C, Senellart P, Lemaıtre A, Sauvan C, Hugonin J, Greffet J J and Bellessa J 2015 *ACS Photonics* **7** 842–8
[38] Huang J, Hsiao Y, Lin Y, Lee C and Lee W 2016 *Sci. Rep.* **6** 28363